FINAL REPORT

Prepared for
National Aeronautics and Space Administration
George C. Marshall Space Flight Center
Alabama 35812

UCLA-ENG-7296
DECEMBER 1972

DIRECTIONAL SOLIDIFICATION OF EUTECTIC COMPOSITES IN SPACE ENVIRONMENT

A.S. YUE

Contract No. NAS8-26402

UCLA • SCHOOL OF ENGINEERING AND APPLIED SCIENCE

UCLA-ENG-7296
December 1972

DIRECTIONAL SOLIDIFICATION OF EUTECTIC COMPOSITES IN SPACE ENVIRONMENT

Final Report

Prepared For

National Aeronautics and Space Administration

George C. Marshall Space Flight Center

Alabama, 35812

Professor Alfred S. Yue

University of California

Los Angeles, California, 90024

Contract No. NAS8-26402

School of Engineering and Applied Science
University of California
Los Angeles

ABSTRACT

The Ni-Ni_3Ta eutectic and a nickel-base alloy containing 30 wt pct Ta were solidified unidirectionally in an electron beam floating zone melting apparatus. It was found that the volume fraction of the Ni_3Ta phase in the Ni-Ni_3Ta eutectic mixture was increased from 7.6 to 36 volume pct in agreement with the theory as predicted.

Tensile properties of the randomly solidified and unidirectionally solidified Ni-Ni_3Ta eutectic were determined as function of solidification rate and temperature. It was found that the ultimate tensile strength decreased as both the test temperature and solidification rate increased. An elongation of 40 pct was obtained for a nickel-base alloy containing 30 wt pct Ta at room temperature. This unusually large elongation was attributed to the superplastic behavior of the alloy.

The critical currents versus the external fields at 2.5, 3.0, 3.5 and 4.2° for the unidirectionally solidified Pb-Sn eutectic have been measured. The values of critical fields (H_r) at zero critical currents were obtained by extrapolation. From these data, a plot of critical field (H_r) against temperature (T) was obtained. The H_r versus T curve fits into a parabolic equation, $H_r = H_o [1 - (\frac{T}{T_c})^2]$, obtained from an IBM 360 least square program. The critical temperature, T_c, was found to be 6.83°K.

The transition temperature T_c of the same Pb-Sn eutectic has been determined experimentally by cooling and warming the sample. The temperature was monitored with an Allen Bradley 39 ohm carbon thermometer which was calibrated against a T58 He Temperature Scale. The transition temperature was found to be 7.37 ± 0.20°K.

CONTENTS

FIGURES

TABLES

1. INTRODUCTION

A two phase composite material is attractive for structural application, because it consists of a strong brittle phase imbedded in a ductile matrix. The idea is to put dissimilar materials together to achieve a new material whose properties are different from any of its constituents. A composite with a phase aligned in the form of thin long fibers is known as a fiber composite. In a fiber composite, the fibers could be continuous or discontinuous along the load axis. In recent years, it has been shown[1] that fibers shorter than the gauge length of a specimen can reinforce a matrix in a manner similar to that of continuous fibers. Jech, Weber and Schwope[2] have shown that the properties of fiber-reinforced composites are essentially the same for continuous and discontinuous fibers. Formerly, it was thought that the fibers have to span the whole length of the specimen for reinforcing the matrix.

Composites have the following excellent properties which make them very attractive for engineering applications, namely:

i) High strength-to-weight ratio.

ii) High stiffness-to-weight ratio.

iii) High strength at elevated temperatures.

1.1 Limitations of Fiber Composites

Preparation of whisker or fiber-reinforced, metallic matrix composites has shown two major problems:

i) Spacing the fiber uniformly over the matrix and aligning them unidirectionally involve a tedious handling task.[3]

ii) Due to weak interfacial bond strength between the fiber and the metal matrix, composites exhibit considerably lower strengths than those predicted by the law of mixtures.[4]

1.2 Controlled Solidification of Eutectic Mixtures

Composites can be manufactured by physically mixing fibers or whiskers in a suitable matrix. Drawbacks of this process have been listed above. However, these difficulties can be eliminated by growing fibers directly in a metal matrix by controlled solidification.[5,6]

Controlled solidification of eutectic mixture produces a well defined two phase microstructure. Regulated direction of heat flow during solidification of eutectic alloys results in the growth of a second phase in a regular form such as rods or platelets aligned in a matrix of the other phase.[7,8] This is accomplished by unidirectionally solidifying eutectic alloys. A planar liquid-solid interface is maintained and a thermal gradient is established in the liquid ahead of the advancing interface during solidification. The phases then grow perpendicular to the planar interface so that they are aligned throughout the rod. Lemkey and Kraft[9] have shown that fibrous phase grown in a unidirectionally solidified eutectic is a true whisker and exhibits high strength.

1.2-1 Advantages of Unidirectionally Solidified Composites

i) They have high interfacial bond strength between the metal matrix and the fiber phase.[10,11]

ii) They are stable at elevated temperatures.[12,13]

iii) Fibers are uniformly distributed in the metal matrix.[14]

iv) Handling problem of fibers is eliminated, thus avoiding damage to them.

v) No separate process is needed to manufacture fibers.

vi) Finally, the process is continuous and thus economical.

1.2-2 Limitations of Unidirectionally Solidified Composites

i) Volume fraction of the fiber phase cannot be increased because it is fixed by the phase diagram.

ii) Only samples of simple geometrical shapes can be made by this technique.

1.3 Mechanism of Fiber Reinforcement

The ultimate tensile strength of a composite is dependent on the following factors:

i) Stress-strain relations of the individual components.

ii) Volume fraction of the fiber phase.

iii) Length to diameter ratio of the fiber phase.

iv) Working temperature.

In case of continuous fibers, the tensile strength σ_c of a composite is given by

$$\sigma_c = \sigma_f V_f + \sigma'_m (1 - V_f) \tag{1.1}$$

where

V_f = volume fraction of fibers

σ_f = tensile strength of fibers

σ'_m = tensile stress of the matrix at fibers failure.

Similarly, the Modulus E_c of the composite is given by

$$E_c = E_f V_f + \left[\frac{d\sigma}{d\varepsilon}\right]_\varepsilon (1 - V_f) \tag{1.2}$$

where

E_f = modulus of the fibers

$\left[\frac{d\sigma}{d\varepsilon}\right]_\varepsilon$ = the slope of the stress-strain curve of the matrix material at the appropriate strain.

At low volume fractions, the composite strength is not given by equation (1.1) because fracture of the fibers does not lead to immediate failure if the matrix can work harden sufficiently. Therefore, equation (1.1) is obeyed only if the composite strength σ_c given by equation (1.1) is higher than the ultimate tensile strength of the matrix, i.e.,

$$\sigma_c > \sigma_u (1-V_f) \tag{1.3}$$

where

σ_u = ultimate strength of the matrix.

Combining equations (1.1) and (1.3), yields the minimum volume fraction V_{min} for which equation (1.1) is applicable.

$$V_{min} = \frac{1}{1 + \frac{\sigma_f}{\sigma_u - \sigma'_m}}$$

For significant increases in composite strength, the volume fraction of the fiber must be higher than V_{min}.

1.4 The Purpose of this Report are:

i) To propose a theoretical model which would predict how volume fraction of the strong fiber phase can be increased by eutectic solidification in the presence of temperature and concentration gradients.

ii) To evaluate the compressive, tensile and high temperature creep properties at room temperature and elevated temperatures.

iii) To measure the superconducting property of the Pb-Sn eutectic.

As shown earlier, the strength of a composite is determined by the stress-strain relationship of its individual constituents. Variation in temperature affects the properties of the composite elements and

therefore the composite strength. Since the behavior of the fiber composites is inherently anisotropic, one should take into account the orientation of the fibers in relation to the direction of loading.

One of the purposes of this investigation was to study the composite tensile behavior in longitudinal direction, parallel to the fiber axis, as a function of test temperature. The material chosen for this purpose was the unidirectionally solidified Ni-Ni_3Ta eutectic. The range of temperature from room temperature to 800°C was selected for study.

2. EXPERIMENTAL PROCEDURE

2.1 Alloy Preparation

Experiments to study the effects mentioned in Section 1 were performed on the unidirectionally solidified Ni-Ni_3Ta eutectic of the Ni-Ta system. Composition of the alloy is depicted in Fig. 1.

Nickel and tantalum of 99.99 pct purity were obtained from Research Organic Inorganic Company. Tantalum was obtained in the form of sheared strips and nickel was in 0.040 in. diameter wire. Nickel-base alloys containing 30 and 37 wt pct tantalum were prepared and melted in a cold hearth, inert electrode, inert atmosphere arc furnace made by Zak Machine Works, Inc., Troy (Green Island), New York, as shown in Fig. 2.

Nickel and tantalum chips were placed in a button-shaped cavity and the furnace was evacuated and flushed with Argon 3 to 4 times. The initial arc was started over a tungsten button in the hearth and then taken over the metallic charge. Input load was controlled with a foot pedal. The alloy button so obtained was flipped a number of times and remelted each time in order to obtain a homogeneous button. After about 5 to 6 flippings the button was taken over to a 1/4 in. by 1/4 in. by 6 in. rod slot and melted in order to give a stock of that size.

Rods were ground and etched to remove any surface impurity prior to unidirectional solidification.

2.2 Solidification

Samples of Ni-Ni_3Ta eutectic were grown from 1/4 in. diameter rods in a Materials Research Corporation electron beam floating zone refiner, Model V4-EBZ-6000, Figs. 3 and 4. The scanner assembly consisted of a specimen, V-groove mounts and an electron beam gun attached to a

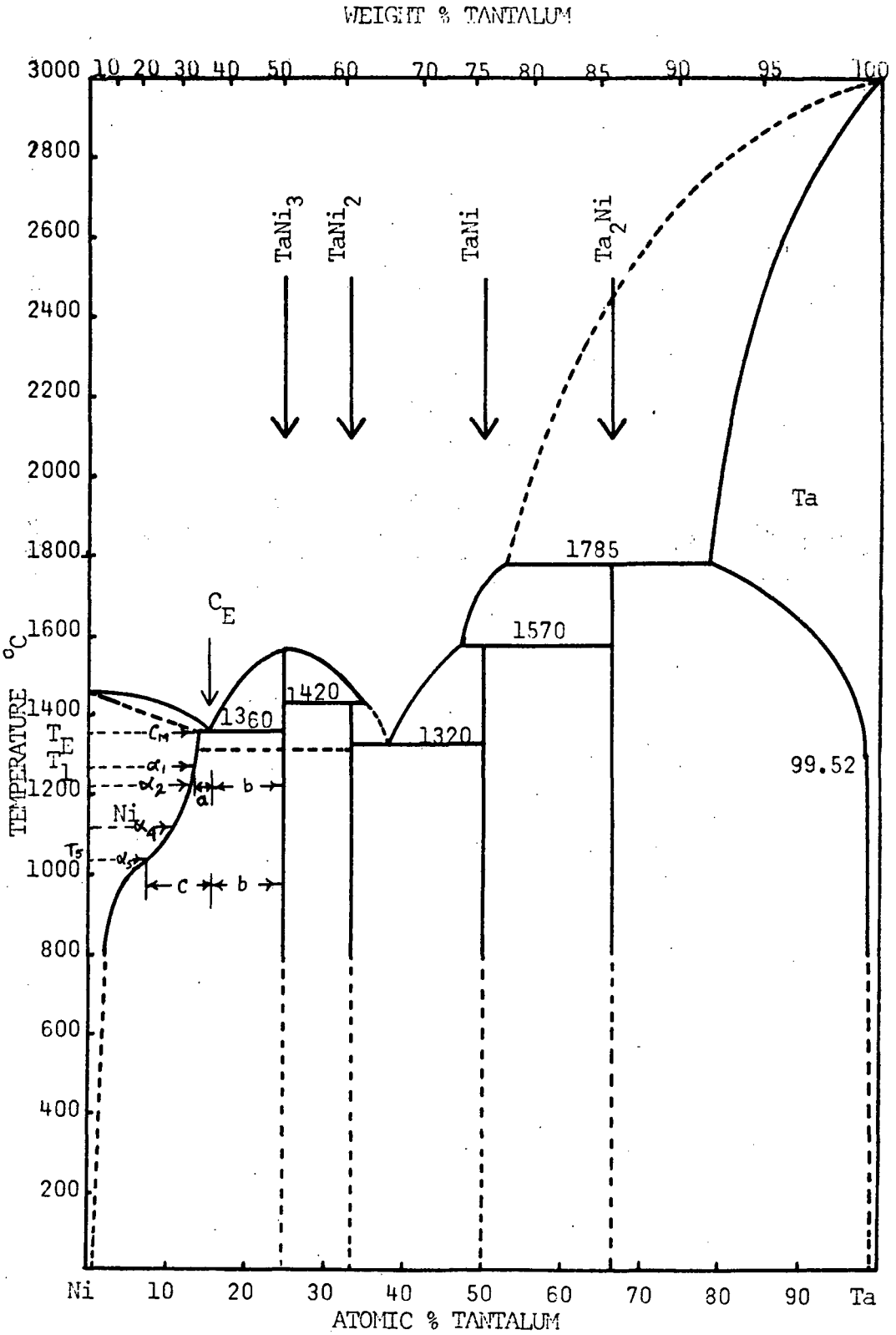

Figure 1. Nickel - Tantalum Phase Diagram

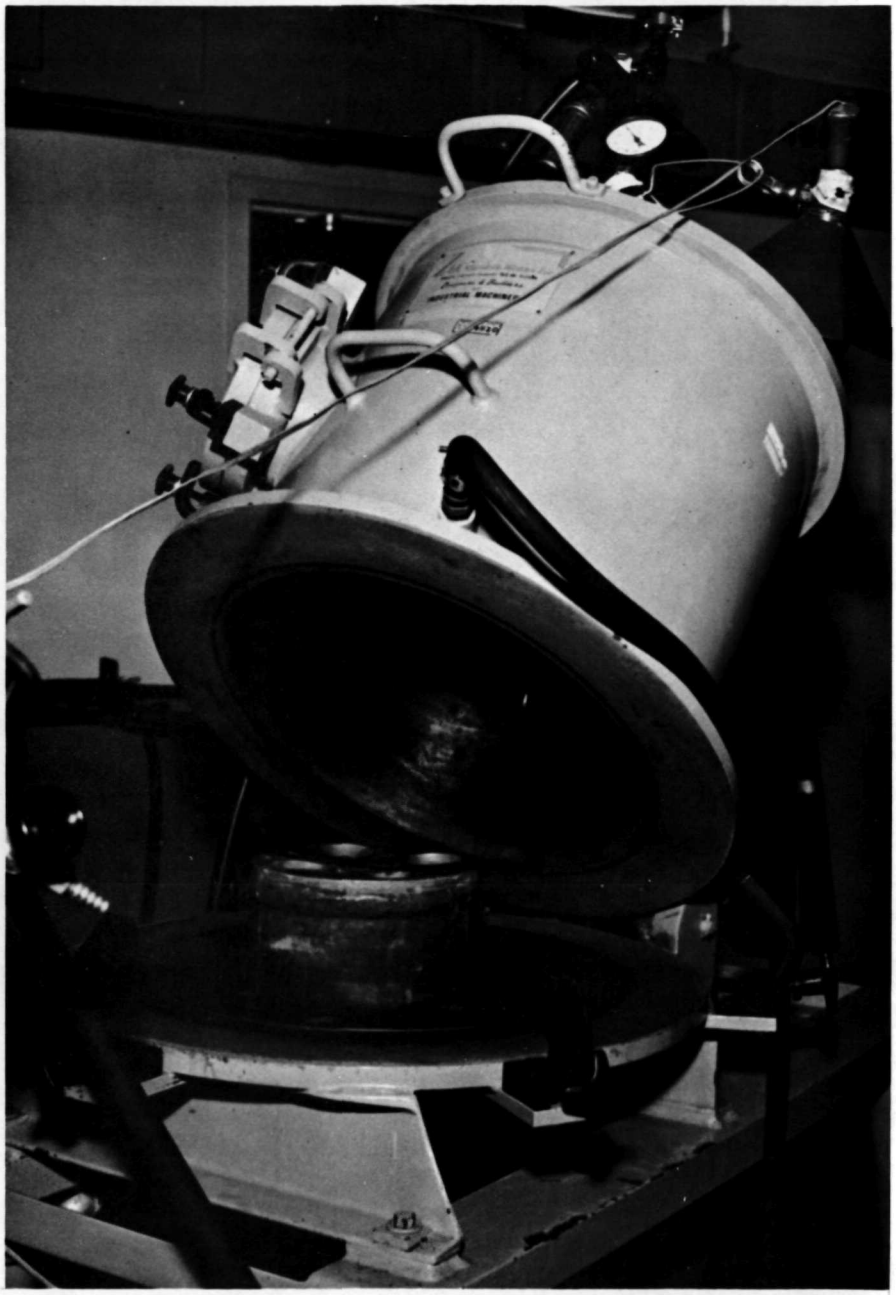

Figure 2. Inert Atmosphere Arc Furnace

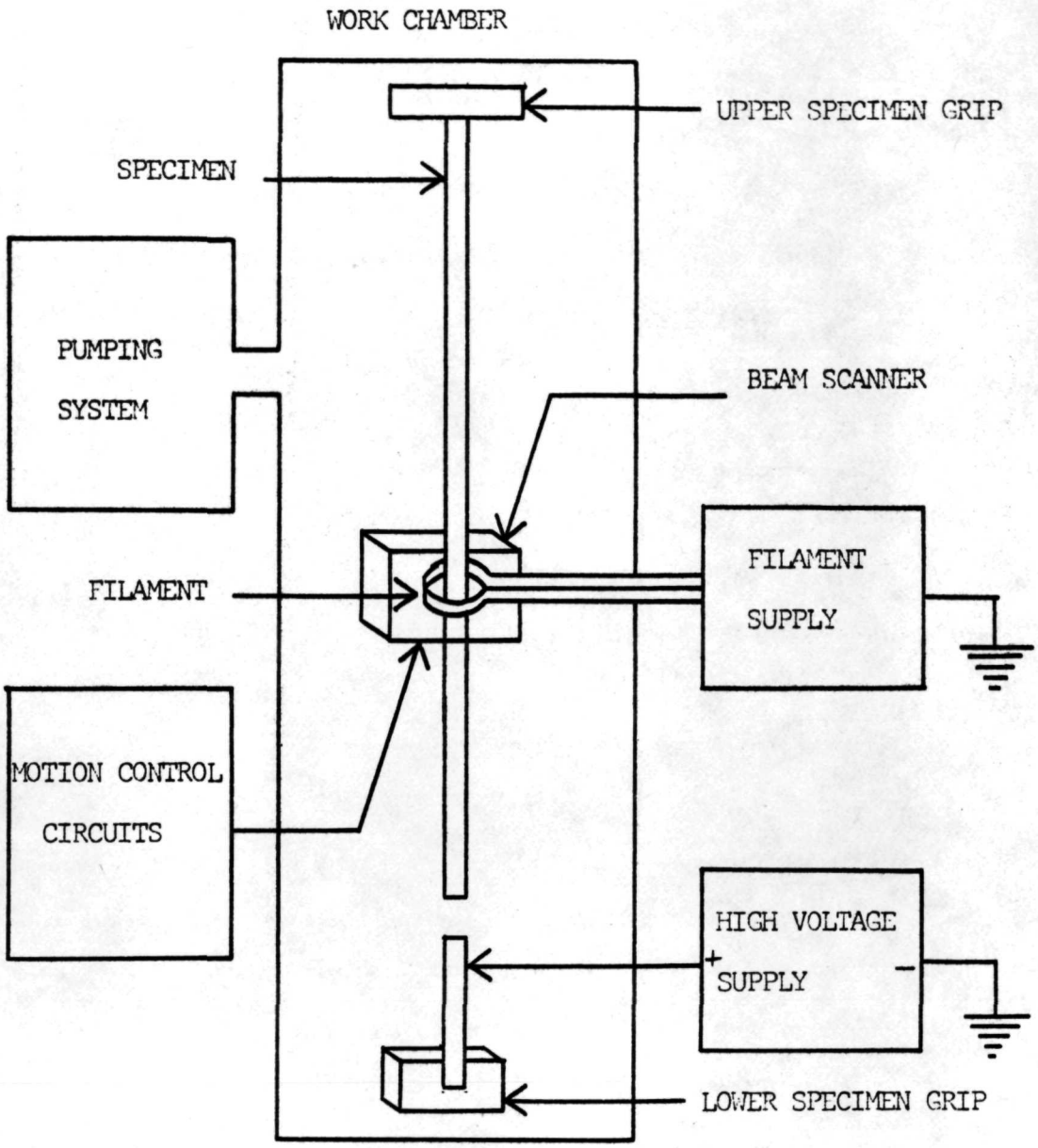

Figure 3. Schematic Diagram of EBZ 6000 Electron Beam Zone Melter

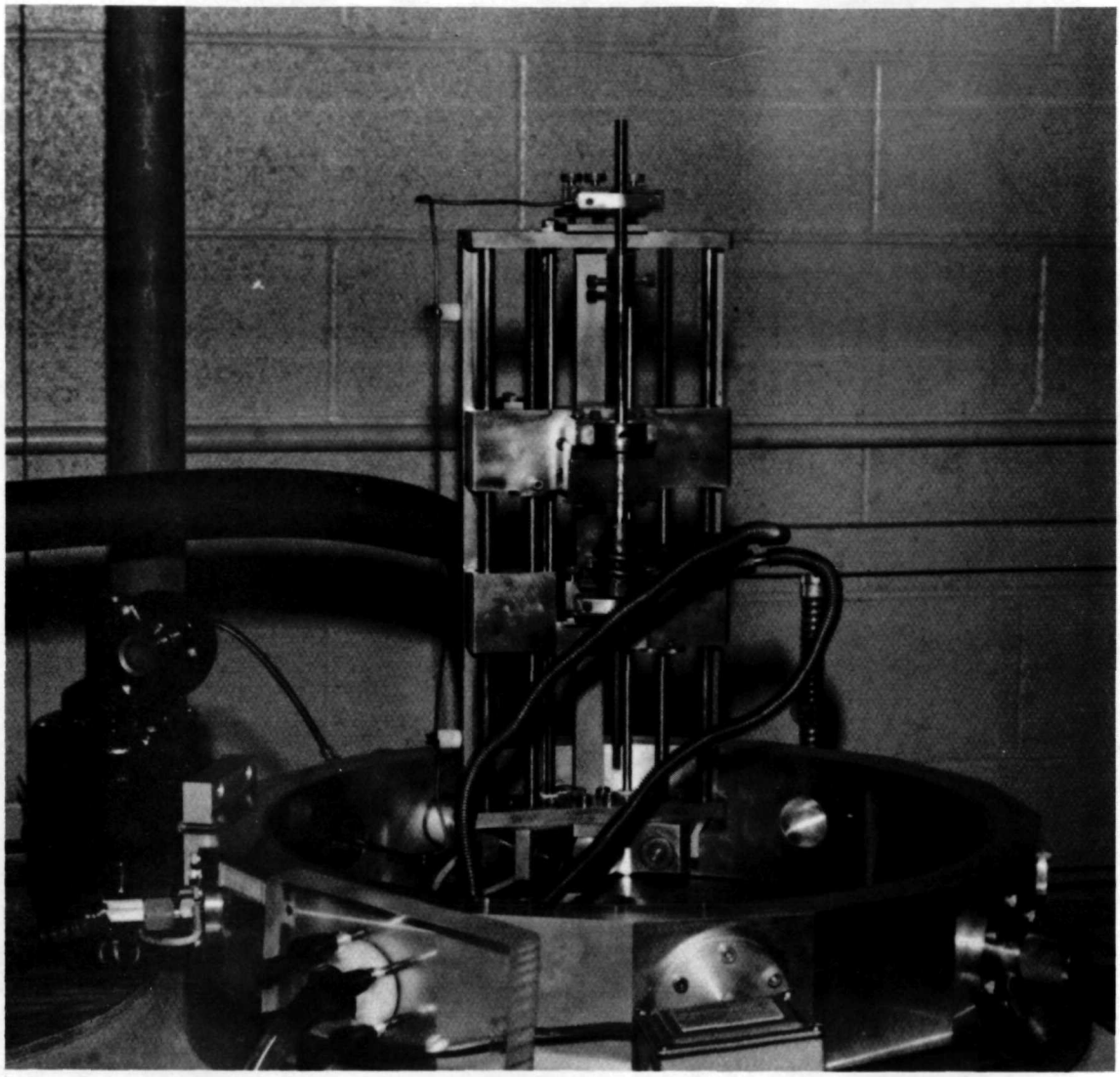

Figure 4. Electron Beam Zone Refiner

stage that moved the gun vertically and parallel to the specimen axis. The electron gun was composed of a 0.625 in. diameter annular filament of 0.032 in. diameter tungsten wire enclosed in a beam focussing pill box. The focussing device design consisted of two grounded molybdenum annular plates 0.375 in. apart with an aperture diameter of 0.375 in. The upper specimen mount was fixed in position while the lower mount was adjustable from outside the vacuum chamber. The scanner assembly was enclosed by a gasket-fitted glass bell jar which rested on an aluminum base. The chamber was evacuated through a liquid Nitrogen cold trap and a water-cooled copper baffle on a 4 in. diffusion pump backed by a 'Welch' mechanical pump. The vacuum chamber was maintained around 2 to 3 x 10^{-6} torr during a run. The electron beam power supply, Materials Research Corporation Model V4-6000, provided voltage up to 5 KV, and current up to 450 milli-amperes.

The Pb-Sn eutectic was solidified in a resistance-wound furnace at a freezing rate of 1.00 cm per hour and under an argon atmosphere. Before solidification, the surface of the rod was cleaned with an etchant. The starting stock was in two pieces, one about 6 in. long which was mounted in the top grip, and a small piece of about 1.5 in. in length was mounted in the lower grip. The lower grip was made of copper with a provision for water cooling through flexible copper tubing. The copper tubing was taken out of the vacuum system through a Teflon block to prevent grounding of the high potential which was present in the pipes during the run. The two outlets of the tubing were connected to a pump and water reservoir with a 'Tygon' tubing, 0.25 in. I.D. Deionized water was circulated in the closed system.

Prior to solidification, the filament was kept level with the lower tip of the upper specimen. The upper tip of the lower specimen was about 1/4 in. below the filament. Following alignment of the rod and the filament, the bell jar was placed over the assembly and evacuated.

For the 0.25 in. diameter rods, the electrons, emitted by the tungsten filament, were accelerated towards the rod by a 2 KV potential difference giving a beam current of 60 milli-amperes. Melting occurred because the emitted electrons, in striking the rod converted their kinetic energy into thermal energy according to the following equation,

$$E = \frac{1}{2} mv^2 N \qquad (2.1)$$

where

E = energy input to the sample

m = mass of one electron

v = velocity of the electrons

N = total number of electrons bombarding the specimen

The gun was positioned so as to melt only the lower end of the upper rod, causing it to fuse with the upper end of the lower rod. The length of the molten zone, determined by the beam current, the applied potential and the beam focussing pill box design, was maintained approximately 3/8 in. The zone travel speed varied from 0.300 in. to 0.600 in. per hour.

All the sample rods were scanned upwards only because of a more stable molten zone. The speeds employed have been mentioned in the previous paragraph.

2.3 Mechanical Testing

2.3-1 Tension Testing

Tension tests were performed on an Instron testing machine of 10,000 pounds capacity. A loading rate of 0.005 in./min. was used.

Round bar tensile specimens with 1.0 in. gauge length were used, Fig. 5. Samples were made by grinding as the material was too hard to machine. The diameter of the specimen was 0.125 in.

The grips that held the specimen were made of Inconel 700. The upper grip was held through a universal joint in order to achieve pure axial load.

Required test temperatures were obtained by resistance-wound Marshall 'clam shell' furnace. The specimens were held at temperature for 30 min. before pulling to failure. The 'OFF' and 'ON' type temperature controller, manufactured by Instron, was used. Two Platinum-Platinum Rhodium thermocouples were used. One was connected to a temperature controller and the other to a potentiometer for measuring the temperature near the specimen.

Young's Modulus of the Ni-Ni_3Ta eutectic was determined by using ultrasonic method. The sample was ground at the ends to make the ends exactly parallel. Two quartz transducers, one on each side, were glued with an epoxy type Armstrong C-2 and 6% activator, by weight. It was then hardened and cured at 77°F for 2 hours. Ultrasonic waves were passed through the sample and the resonance frequency was determined. Knowing the length of the specimen the wave length was determined and thereby the velocity, by the formula

$$\lambda = \frac{v}{f} \qquad (2.2)$$

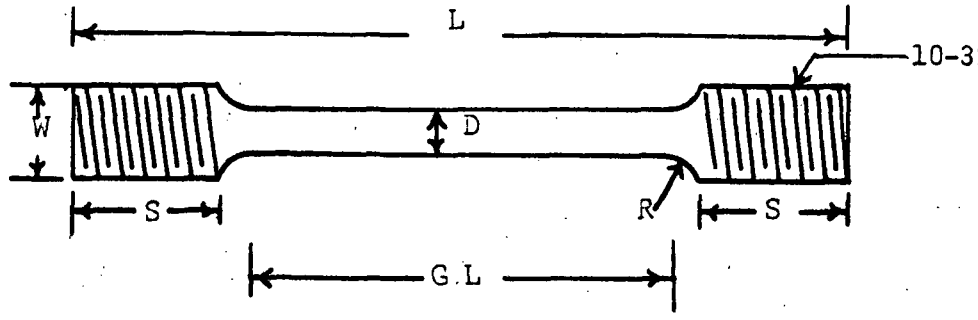

L = 2.0 inches

D = 0.125 ± 0.001 inches

S = 0.50 ± 0.005 inches (Threaded)

G L = 1.0 ± 0.005 inches

W = 0.20 inches

R = 3/32 inches (Fillet radii)

Figure 5. Tensile Specimen

where

λ = wave length

v = velocity

f = frequency

$$E = \rho \cdot v^2 \qquad (2.3)$$

where

E = Young's Modulus

ρ = density of the alloy

v = velocity

By knowing the density and velocity, E was determined.

2.3-2 Compression Test

Tests were performed on 1/4 in. by 1/4 in. by 1/2 in. long specimens on the Instron machine. Two Alumina rams were used for compression at 400°C. Tests were discontinued as the rams gave way before the samples. Here also, the specimens were ground due to poor machinability of the material.

2.3-3 Creep Test

Creep specimens, 1 in. gauge length and 1/8 in. in dia., were made from unidirectionally solidified Ni-Ni_3Ta ingots, 1/4 in. in dia. and 2 in. long. These specimens were tested in a constant load creep machine. Since the elongations of the specimens are small under load, these creep testings were considered as constant stress experiments.

A resistance-heated split furnace was used and the test temperatures were controlled to an accuracy of $\pm$ 7°F. Elongation of the specimens were measured by recording the lever-arm displacement. This displacement was measured by a dial gauge indicator and was recorded continuously

using a cantilever beam with two strain gauges on both sides of the specimen. The longest time for a test was restricted to 250 hrs. Specimens that did not fail within this time limit were removed or retested at a higher temperature or a higher stress.

2.4 Scanning Electron Microscope

After the tension test, the fractured surface was examined under a scanning electron microscope. The microscope basically consists of high voltage supply, filament supply, lense control supply, and electron collector. Secondary electron emission from a specimen, caused by scanning it with an electron beam, is used to reproduce topographical details.

2.5 Transmission Electron Microscope

A Hitachi electron microscope, type HU-11 was used for thin film work. Thin slices were cut from many directionally solidified Ni-Ni_3Ta eutectic with a 'Servo Met' oil-immersed spark cutter. Thin discs of 1/8 in. diameter were reduced to 0.010 in. by mechanical polishing on emery papers. The thin foils were then jet-polished using the following solution:

Methanol	-	93 ml
Sulphuric acid	-	5 ml
Hydroflouric acid	-	1.25 ml
Voltage	-	80 volts
Temperature		< 20°C

After standardizing, it was determined that about 12 seconds of jet was required to remove 0.001 in. of material from the specimen at 80 volts. The foils were then electropolished with the same solution at liquid nitrogen temperature, in order to reduce the overall thickness

to produce a very thin section in the middle of the foil and a perforation to obtain diffraction patterns.

2.6 Microscopic Examination

After mechanical testing, all specimens were examined with a light microscope along their longitudinal axes to determine their modes of fracture. Specimens were etched for about 5 seconds in the following solution:

Hydrochloric acid - 30 ml

Hydroflouric acid - 16 ml

Water - 120 ml

Ferric Chloride - 6 gms

Photomicrographs were taken with a Bausch and Lomb microscope with P/N 55 type of Poloroid film.

2.7 Superconductivity Measurement

A unidirectionally solidified Pb-Sn eutectic sample, 1/8" in dia. and 1-1/4" long, was clamped with OFHC copper cylinders to eliminate local heating. Potential taps were first wrapped on the sample and then were glued with silver epoxy.

The sample current was increased to a pre-set value, using Kepco MP-10 Programmer to control the Harrison 6260 A dc current power supply as shown in Fig. 6. The sample current was measured by reading the voltage with a Dana 4470 digital voltmeter across a series standard 10 milli-ohm resistor.

The sample voltage was amplified through a Keithley 148 nanovoltmeter The amplified signal was fed into the Y-terminal of a Mosley 7000 A X-Y recorder and the X-terminal of the recorder was used to record the external magnetic field which was increased very slowly and steadily by using a Kepco MP-10 programmer. The magnet current was monitored

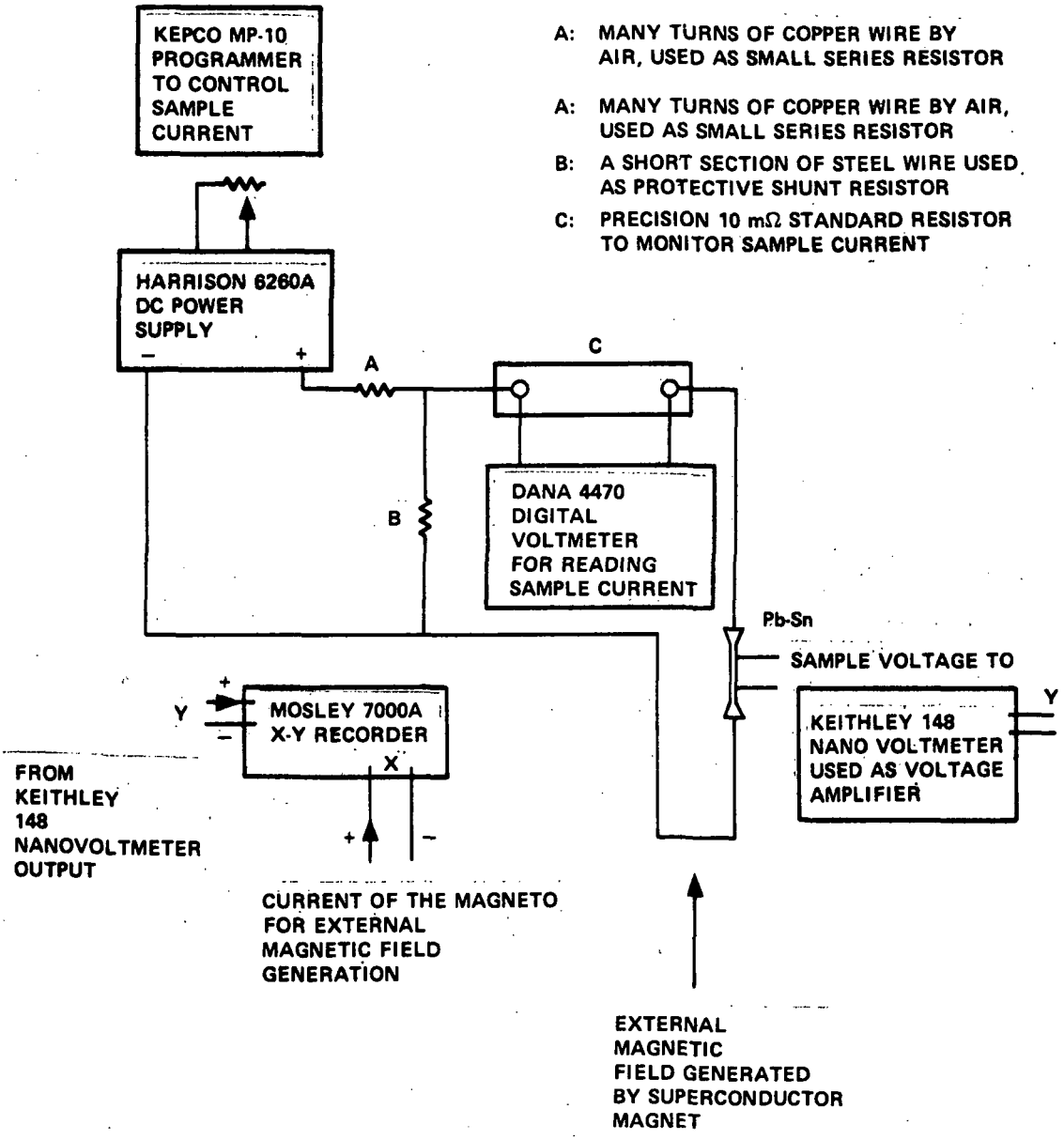

Figure 6. Circuitry for Sample Voltage, Current Measurement.

by detecting the voltage across a standard 1/2 milli-ohm resistor N as shown in Fig. 7. At a fixed temperature, the sample voltage changes from zero voltage (superconductiving state with zero resistance) to full voltage (normal state with normal residual resistance) when the external magnetic field changes slowly and steadily.

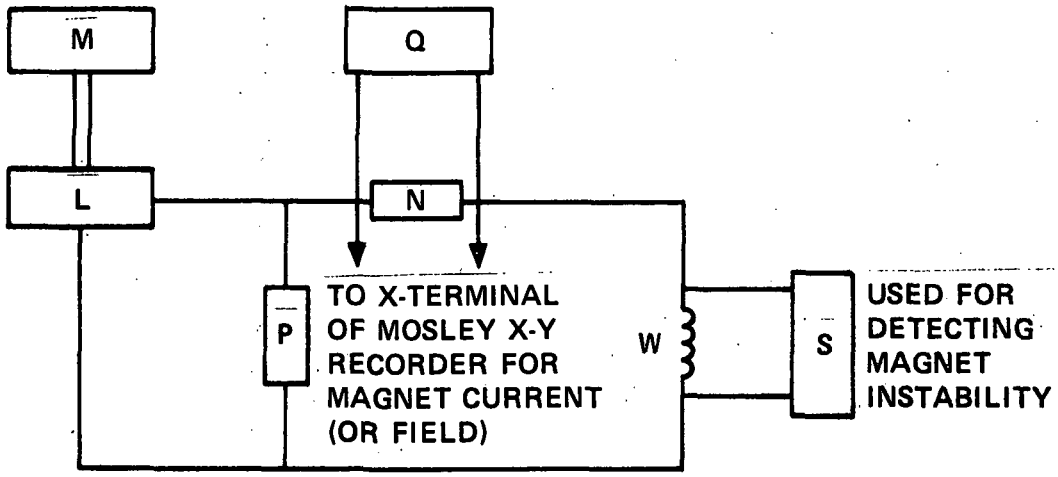

L, Harrison (Hewlett Packard) D.C. Power Supply Model 6260A
M, Kepco Programmer Model MP-10 used to Control the Speed of Magnet Current
N, 1/2 milli-ohm Standard Resistor
P, Protective Shunt Resistor
Q, Fluke High Impedance Voltage-Null Detector Model 845AB
S, Keithley Electrometer Model 610B
W, Superconductor Magnet (Solenoid) NbTi Magnet

Figure 7. Magnet (Solenoid) Circuitry

3. RESULTS

3.1 Eutectic Microstructure

The microsture of the directionally solidified Ni-Ni_3Ta eutectic was characterized by a rodlike Ni_3Ta phase, partially aligned in the direction of solidification. Various solidification rates were employed in order to determine an optimum rate to produce the best microstructure. It was found that the diameters of the Ni_3Ta rods ranged from 10 to 30 microns. Figure 8 shows the longitudinal section of a directionally solidified rod at 0.6 in. per hr. Several studies (15,16) have shown that the microstructure can be altered by varying the temperature gradient and the growth rate.

A volume fraction analysis of many longitudinal sections of specimens by quantitative metallography indicated that the Ni_3Ta fibers comprised of 36 volume pct of the composite while the calculated volume pct of the Ni_3Ta phase at the eutectic temperature (1360°C) of the Ni-Ta binary phase diagram is only 7.6. This increase in volume fraction of the Ni_3Ta phase in the directionally solidified alloy is attributed to the diffusion of tantalum from the saturated nickel-rich solid solution to the preexisting Ni_3Ta rods and the concomitant epitaxial growth of the rods.

3.2 Mechanical Properties of Ni-Ta Alloys

Table 1 summarizes the results of tensile and compressive testing of Ni-Ni_3Ta eutectic at various temperatures.

$E = 28.5 \times 10^6$ psi was determined by the ultrasonic method.

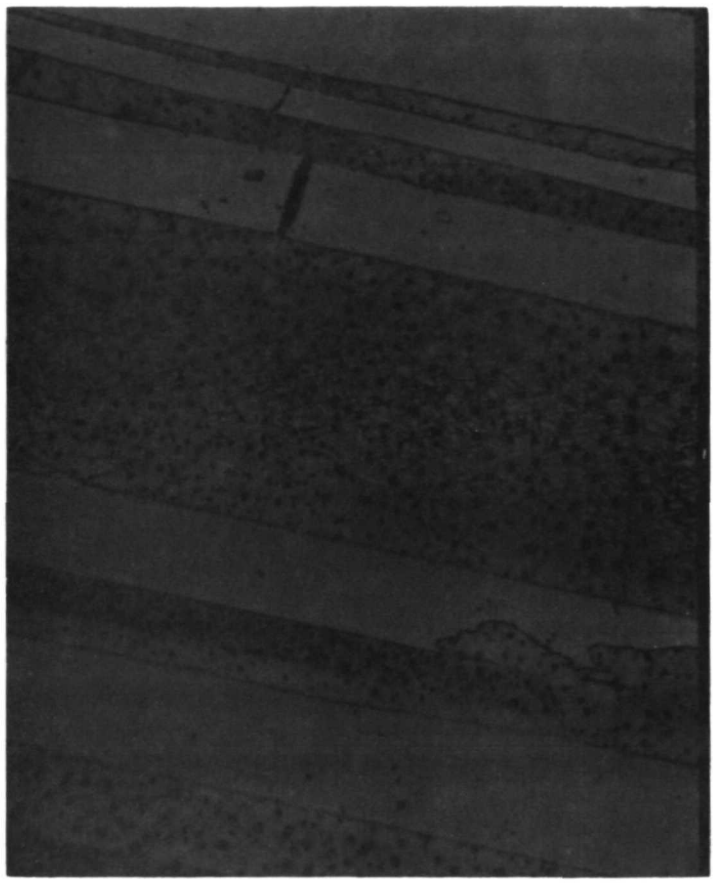

Figure 8. Longitudinal Section of the Directionally Solidified Ni-Ni_3Ta Eutectic.

TABLE I

Mechanical Properties of Ni-Ni_3Ta Eutectic Alloy

Sample and History	Type of Test	Temperature of Test	Ultimate Strength, 10^3 psi	0.2 % offset Yield Strength, 10^3 psi	Fracture Strain, Percent
Randomly solidified	Tension	Room Temperature	61.5	-	0.10
Solidified with water cooling at 0.3 in./hr	Tension	Room Temperature	81.3	80.5	0.29
Solidified at 0.4 in./hr	Tension	Room Temperature	82.0	-	0.127
Randomly solidified	Tension	400°C	80.3	-	-
Solidified at 0.4 in./hr	Tension	400°C	110.7	82.5	1.50
Solidified with water cooling at 0.46 in./hr	Tension	400°C	77.90	-	0.11
Solidified at 0.6 in./hr	Tension	400°C	45.1	-	-
Solidified with water cooling at 0.46 in./hr	Tension	600°C	65.6	-	-
Solidified with water cooling at 0.46 in./hr	Tension	800°C	35.0	-	0.10
Randomly solidified*	Compression	400°C	149.9	-	-

* Experiment discontinued as Alumina rams fractured before the specimen

3.2-1 Tensile Tests

The temperature dependance of stress-strain curve of directionally solidified Ni-Ni_3Ta eutectic is represented graphically in Fig. 9. Additional tensile data at room temperature for Ni-30 wt pct. Ta in the directionally solidified condition is presented in Table 2 and is graphically represented in Fig. 10.

In several tests the directionally solidified specimens fractured within the elastic portion of the stress-strain curve. For such tests only the ultimate strength and elongation at fracture have been tabulated.

Assuming, that there is no plastic deformation in the fibers and that the composite material fractures when the fibers fracture, the elongation in the composite will be equal to the elongation in the fibers and also in the matrix, i.e.,

$$\bar{\varepsilon}_c = \bar{\varepsilon}_f = \bar{\varepsilon}_m$$

The basic equations of a continuously reinforced composites, where both matrix and the fiber are elastically loaded are given by equations 1.1 and 1.2, i.e.,

$$\sigma_c = \sigma_f V_f + \sigma'_m (1 - V_f)$$

or

$$\sigma_f = \frac{\sigma_c - \sigma'_m (1 - V_f)}{V_f} \qquad (3.1)$$

In this equation the value V_f has been determined from the actual photomicrograph (36 pct), σ_c is the ultimate tensile strength of the composite which was 82.0×10^3 psi. σ'_m is the matrix strength 50×10^3 psi at fiber fracture strain (E_f). By inserting these values, the ultimate strength of the fiber was found to be

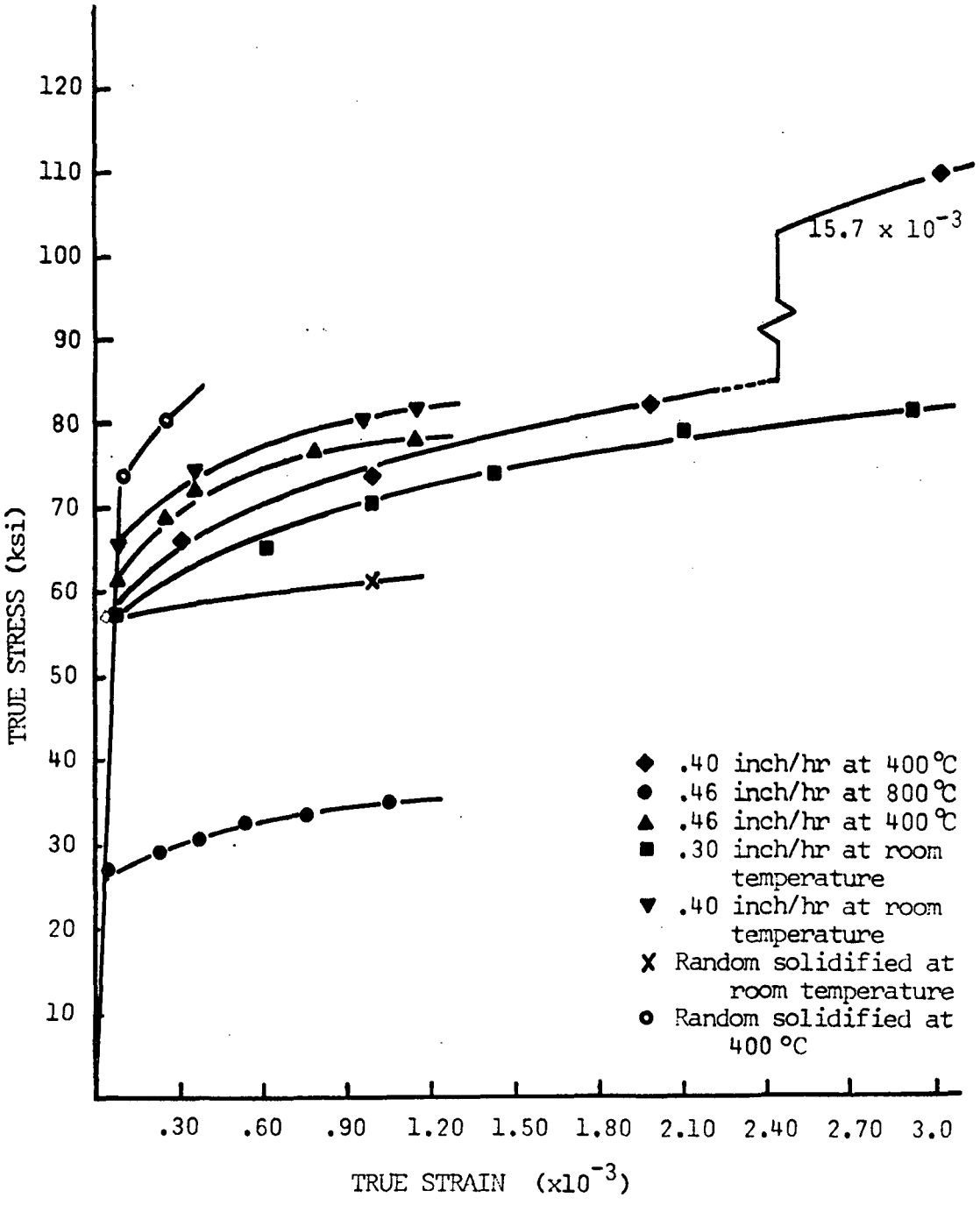

Figure 9. Stress-Strain Behavior of Ni-37 wt pct Ta Eutectic in Tension

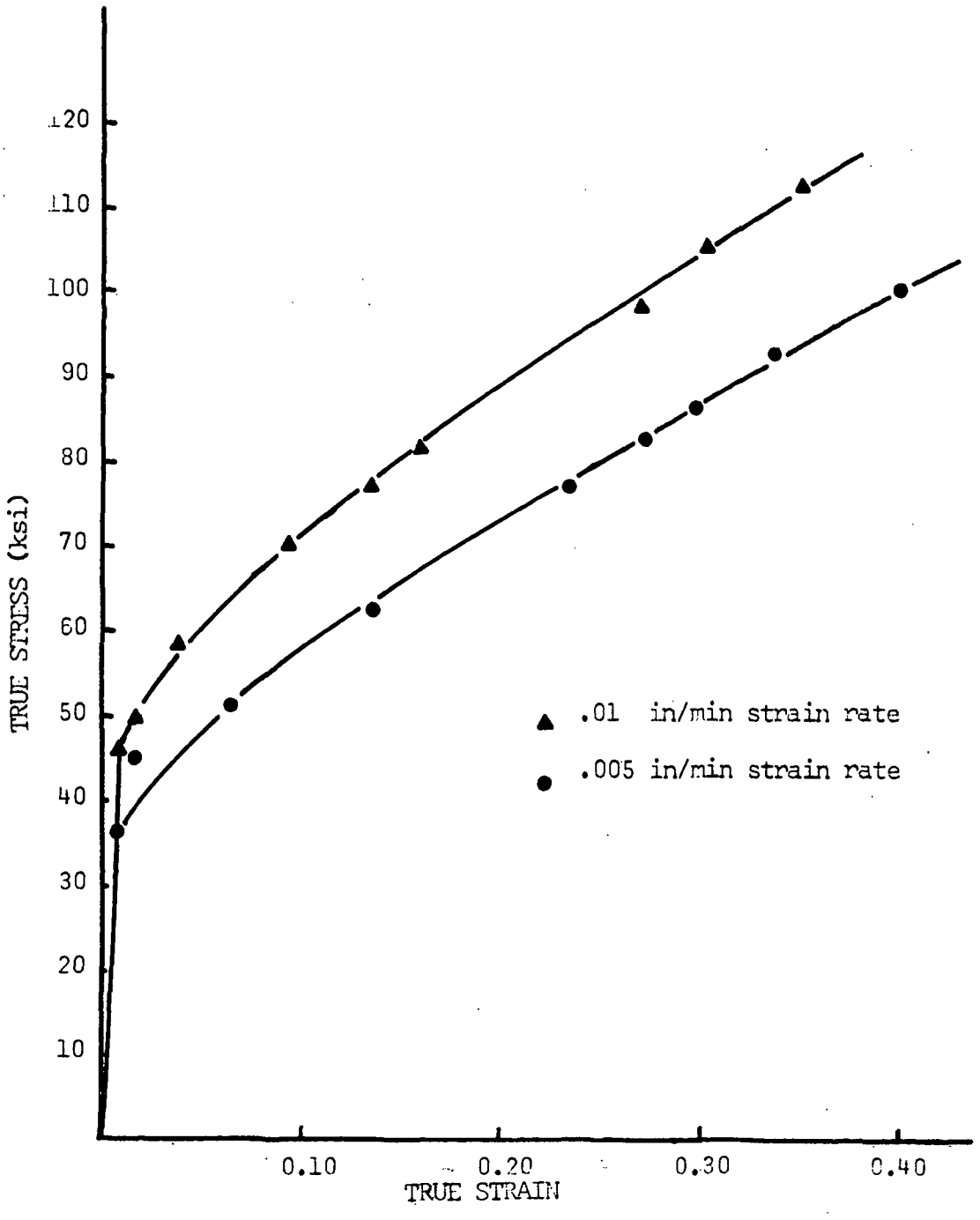

Figure 10. Stress-Strain Behavior of Ni-30 wt pct Alloy in Tension at Room Temperature

$$\sigma_f = 138.8 \times 10^3 \text{ psi}$$

This value is lower than that expected of strong fibers. This is probably due to the presence of defects in the Ni_3Ta fibers.

Fracture in different tensile specimens of directionally solidified eutectic had taken place at different places within the gauge length. Typical examples are shown in Figs. 11(a), (b) and (c) which show practically no necking except in one case where the reduction in area was found to be 0.9 pct at a test temperature of 400°C.

Figure 12 shows the fractured surface of a tensile specimen under a scanning electron microscope. This photomicrograph shows the absence of dimples and the presence of steps. This type of fracture is typical of brittle materials.

As expected, the tensile strength decreases with increasing test temperature. Figure 13 shows the variation of ultimate tensile strength with test temperature for the directionally solidified $Ni\text{-}Ni_3Ta$ eutectic.

Solidification rate also has some effect on the ultimate tensile strength. Figure 14 graphically represents the decrease in tensile strength with an increase in solidification rate. With faster solidification rates, diffusion of Ta atoms to the reinforcing phase is slow and incomplete thus the low strength.

An interesting feature was noticed in the tensile tests of Ni-30 wt pct Ta alloys at room temperature as shown in Fig. 15. The sample elongated about 41 pct and the fracture had occurred without any visible necking. In one of the tests the fractured surface was a knife edge. The average 0.2 pct off-set yield strength was

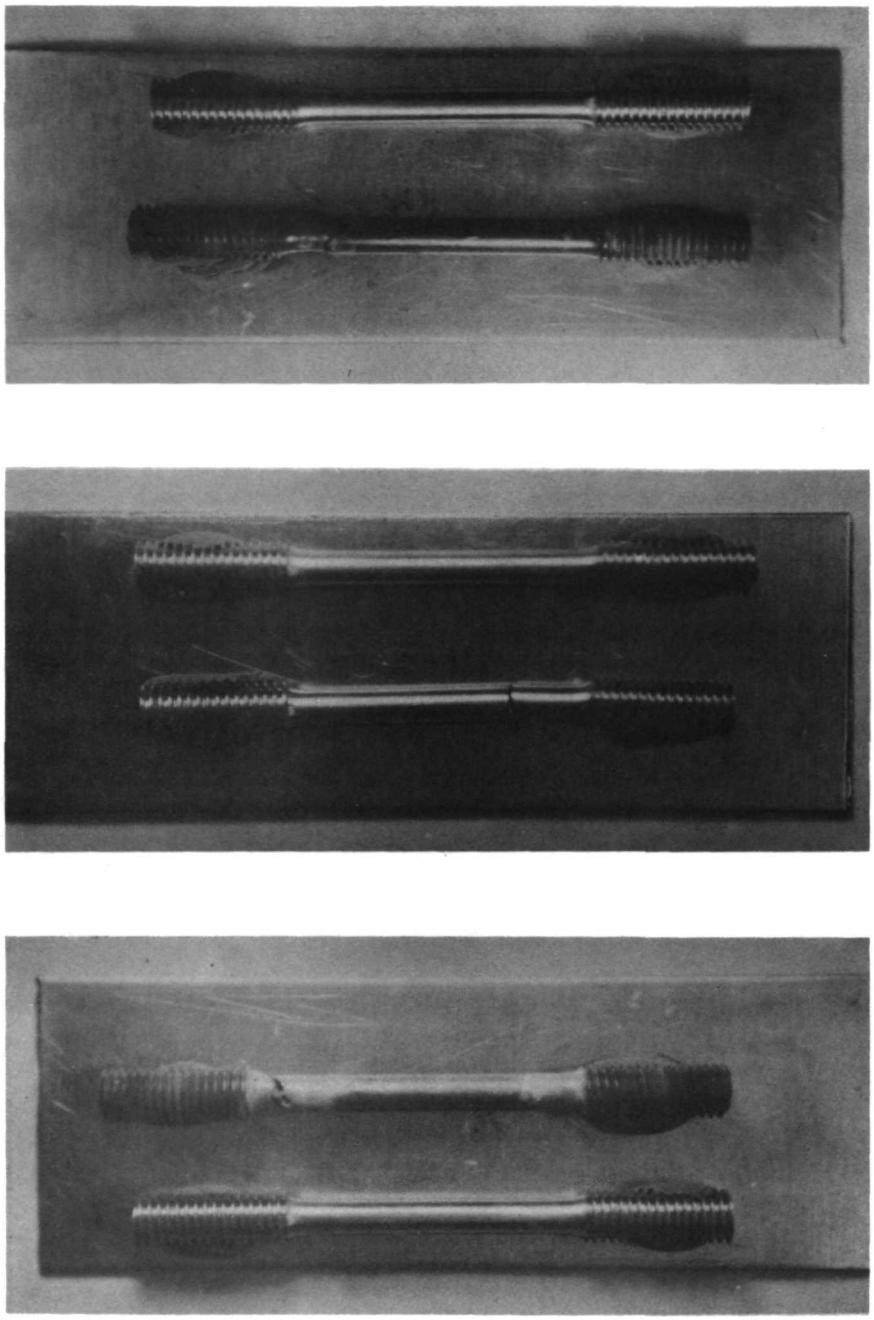

Figure 11. Fractured Tensile Specimens

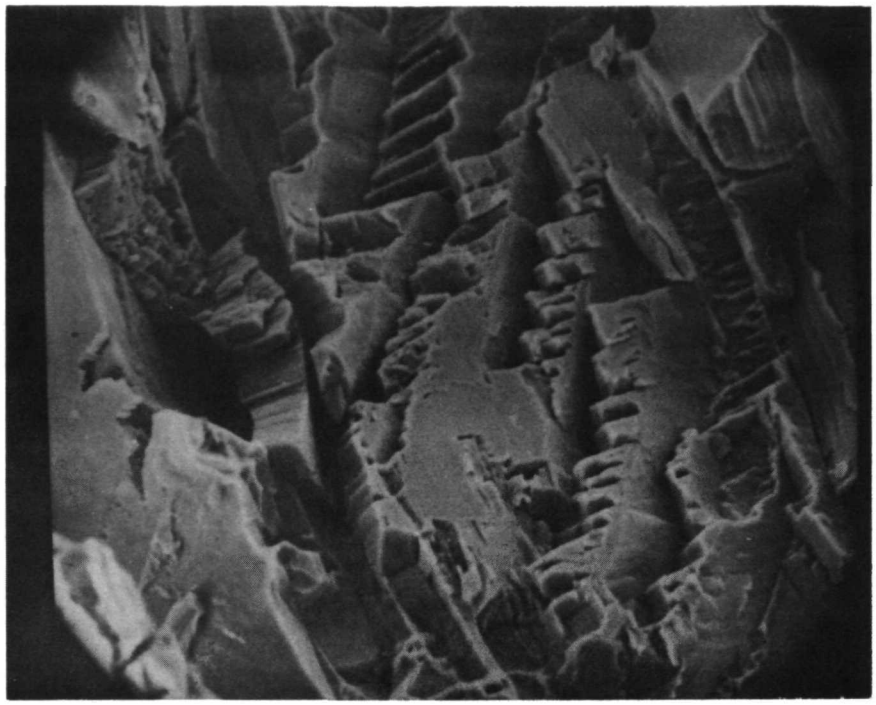

Figure 12. Fracture Surface Under Scanning Electron Microscope.

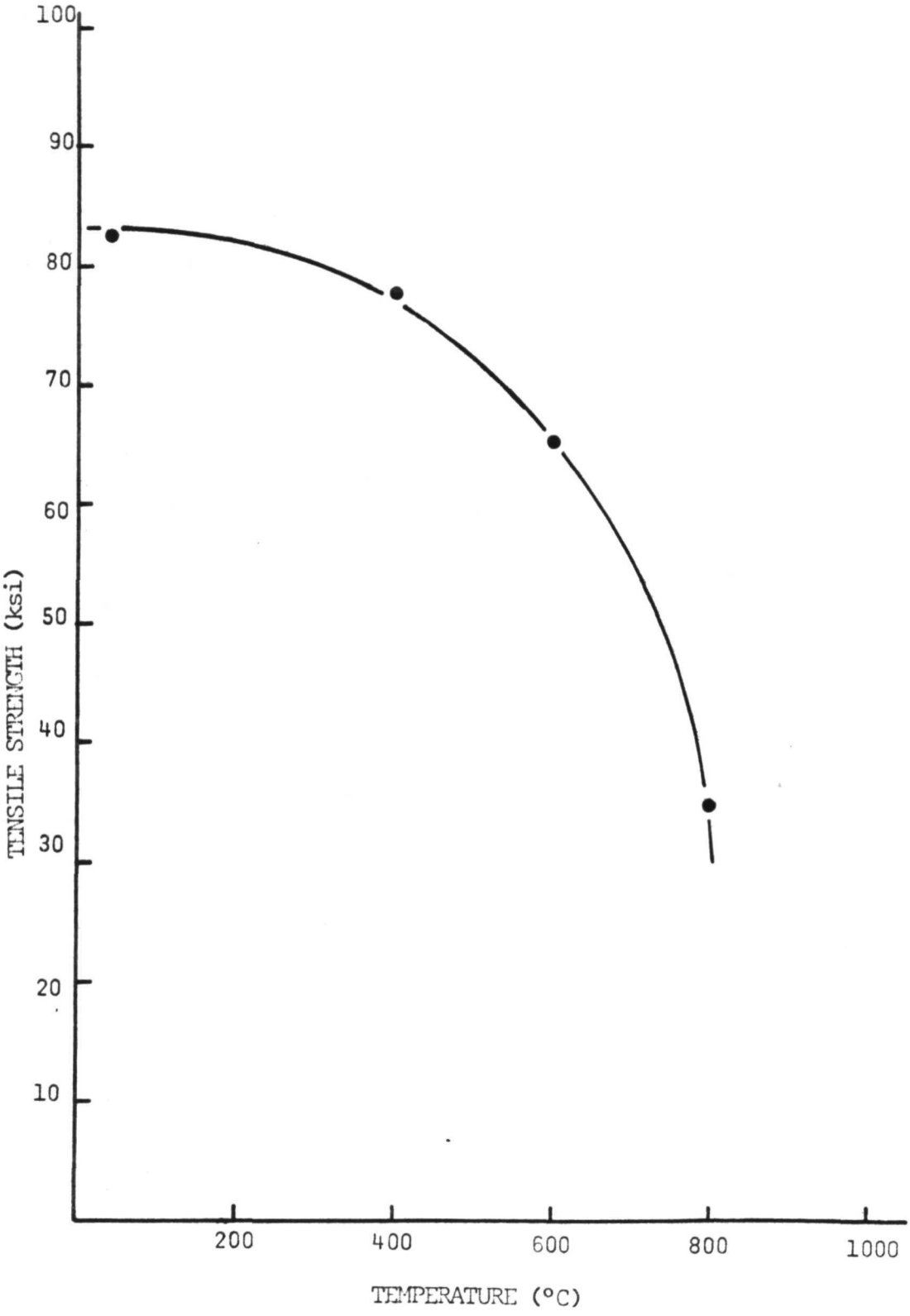

Figure 13. Ultimate Tensile Strength of Ni-Ni_3Ta Eutectic at Elevated Temperatures

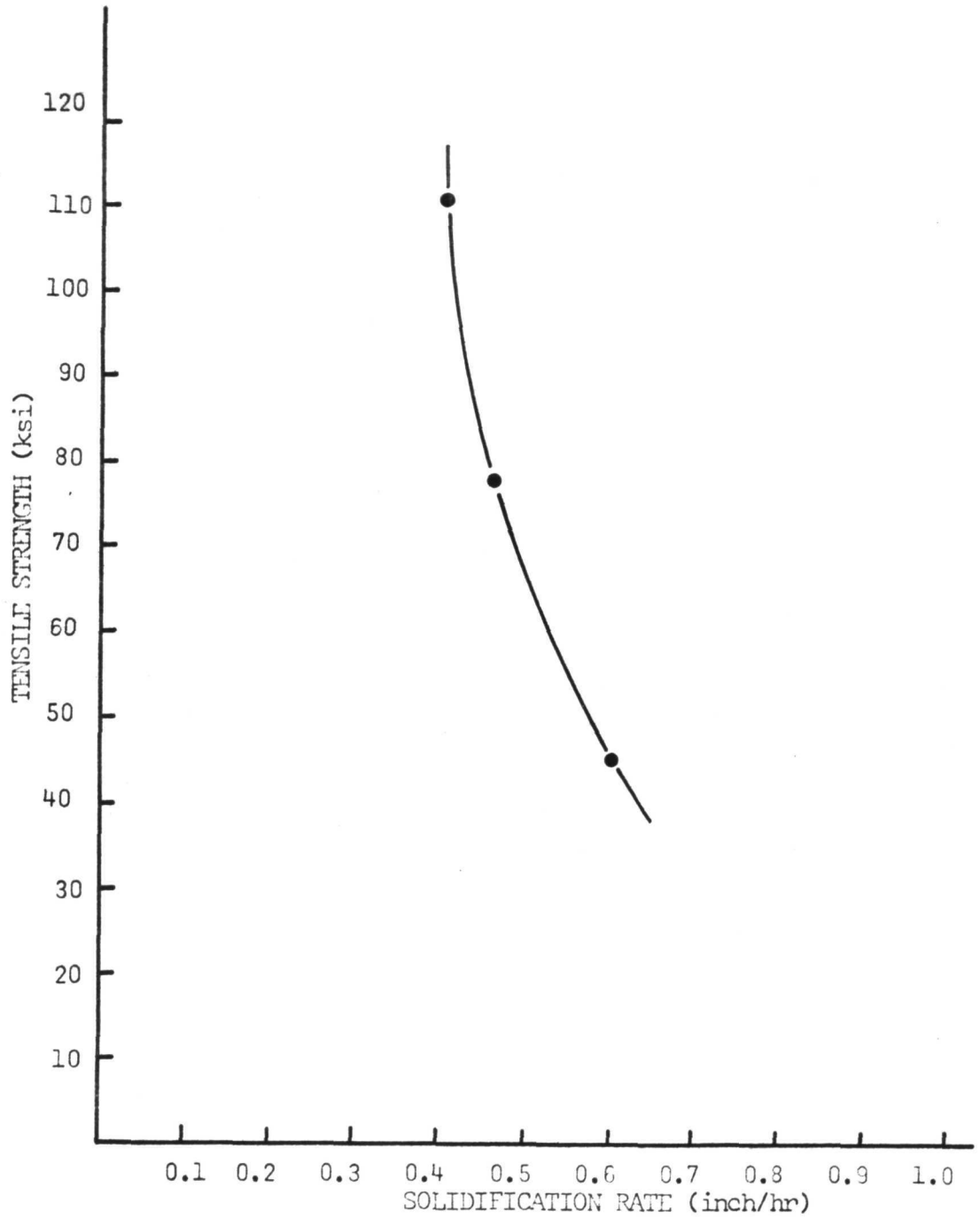

Figure 14. Ultimate Tensile Strength of Ni-Ni_3Ta Eutectic at Various Solidification Rates at 400°C

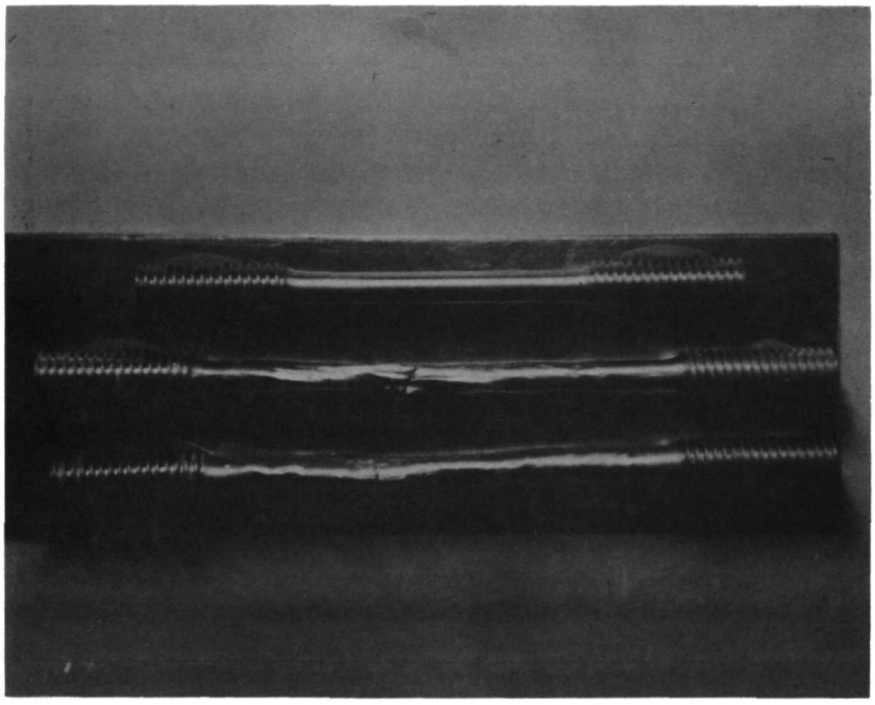

Figure 15. Fractured Tensile Specimen of Ni-30 wt pct Ta.

50.5×10^3 psi.

3.2-2 Compression Test

The compression test on a randomly solidified Ni-Ni_3Ta eutectic was carried out but could not be continued because the Alumina rams fractured during testing. At 400°C the strength noticed at that point was about 150×10^3 psi.

3.3 Transmission Election Microscopy

The thin foils prepared for determining orientation of the Ni-Ni_3Ta eutectic by electron diffraction technique were not of good quality. Too much of oxide formation accompanied electropolishing and as a result good diffraction patterns could not be obtained.

3.4 Creep Property

High temperature creep curves of unidirectionally solidified Ni-Ni_3Ta eutectics are given in Fig 16.

Comparison of curves of specimens tested at the same temperature (1000°F) and the same stress (40Ksi) reveals the prestraining effect, i.e., a specimen that was prestrained at 30Ksi exhibits a lower creep rate in the steady-state region. On the other hand, both specimens tend to elongate equally with increasing time. Whether the prestraining of the specimen would improve the creep resistance can not be established definitely in this study because more experimental data are needed for the proof.

The second or perhaps a more significant result of this study is the temperature sensitivity of the unidirectionally solidified Ni-Ni_3Ta eutectic. Two specimens, tested at 40 Ksi and at 1000° and 1100°F, had no effect on the creep resistance of the specimens. When the test temperature was increased from 1100°F to 1200°F at the same stress level (40Ksi), the specimen failed after 15 hrs. of loading.

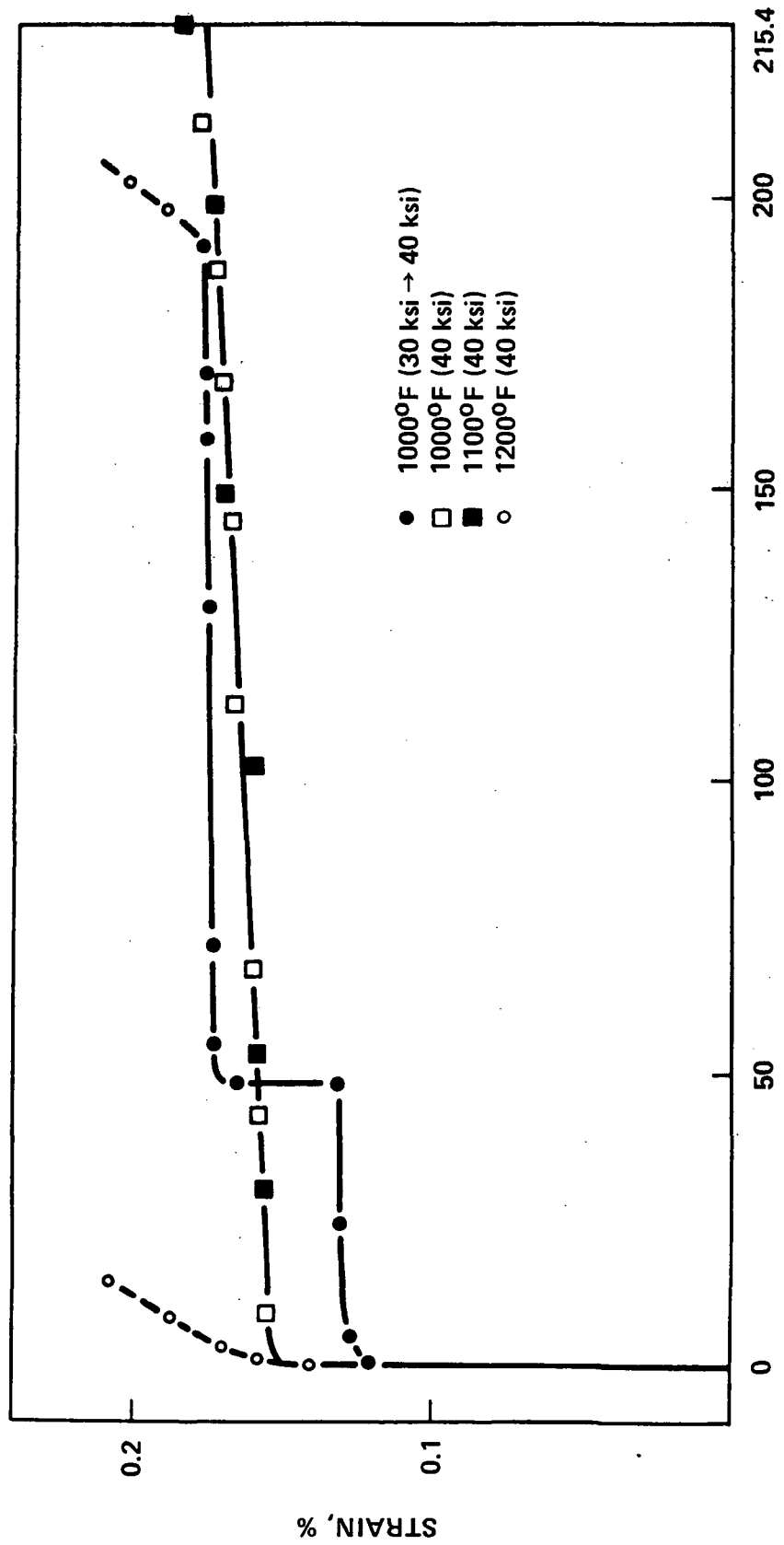

Figure 16. Creep of Ni-Ni_3Ta Eutectic

The same behavior was observed also with a specimen that was prestrained at 1000°F for 192 hrs. and at the same stress level. These results suggest that a critical temperature range above which the creep resistance would be greatly reduced, exists in the unidirectionally solidified Ni-Ni_3Ta eutectic. Based on the experimental data obtained from this study, a critical temperature range is between 1100°F and 1200°F.

3.5 Superconductivity Property

A plot of the critical current (J_c) versus the external magnetic field for 2.5, 3.0, 3.5 and 4.2°K is given in Fig. 17. At the high field region, the extrapolation to zero critical current gives the J_c value of the critical field. This critical field at zero critical current versus temperature is plotted in Fig. 18. The curve is nearly parabolic and can be represented by the following parabolic equation:

$$H_c = H_o \left[1 - \left(\frac{T}{T_c}\right)^2\right]$$

where H_o is the critical field at 0°K and is equal to 1.44 Kg and T_c is the critical temperature and is 6.83°K. The lower values of H_c in Fig. 18 were the start - transition fields and the upper values were the complete normal fields. It can be seen from Fig. 18 that the transition is rather broad and it is completely reversible (no hysteresis as one increases and decreases the magnetic field).

The transition temperature T_c of the unidirectionally solidified Pb-Sn eutectic has been determined experimentally by cooling and warming the sample. The temperature was monitored with an Allen Bradley 39 ohm carbon thermometer which was calibrated against a T58 helium temperature scale. The transition temperature was found to be 7.37 ± 0.20 °K.

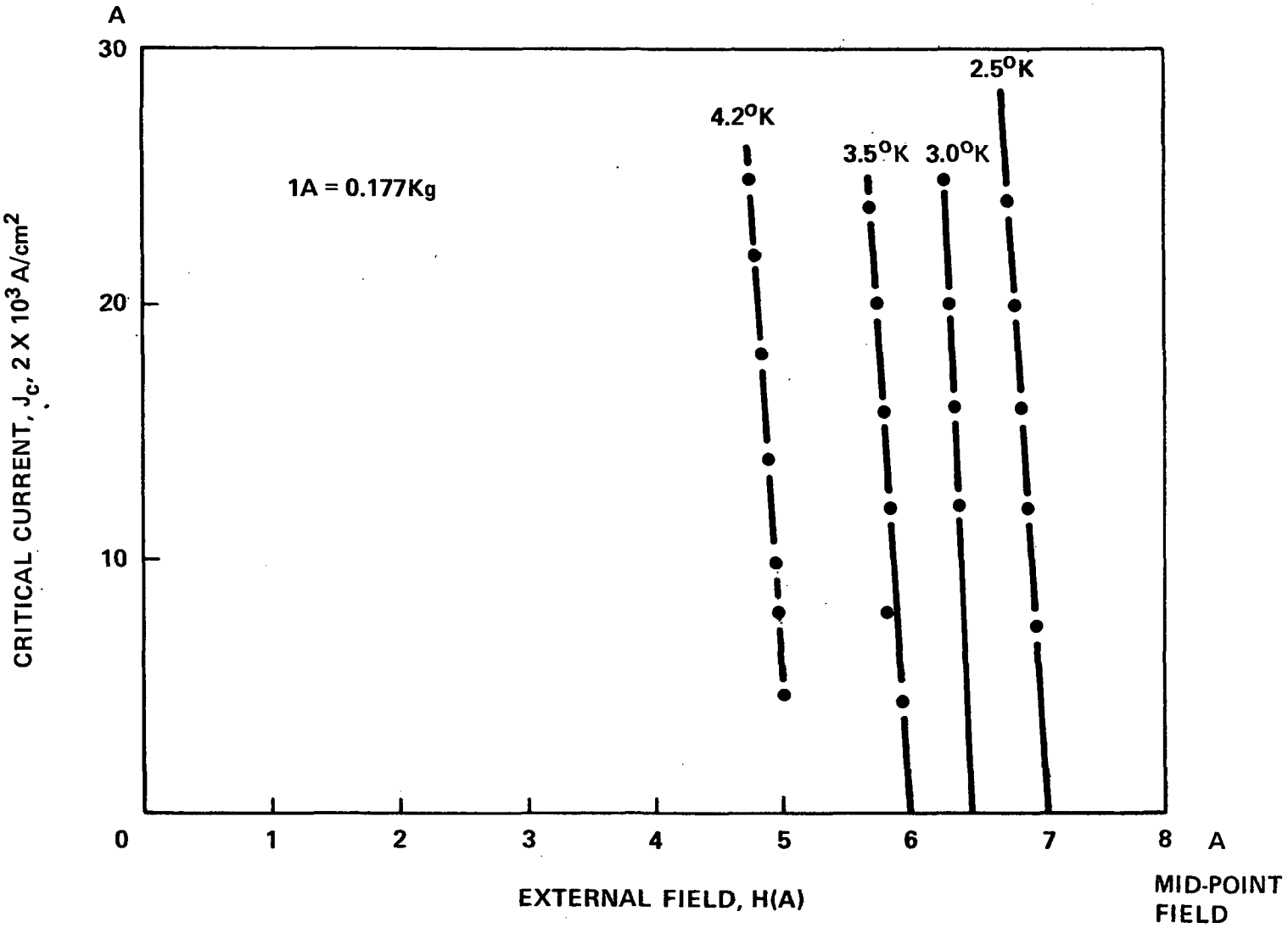

Figure 17. The Critical Current Versus External Magnetic Field at Various Temperature

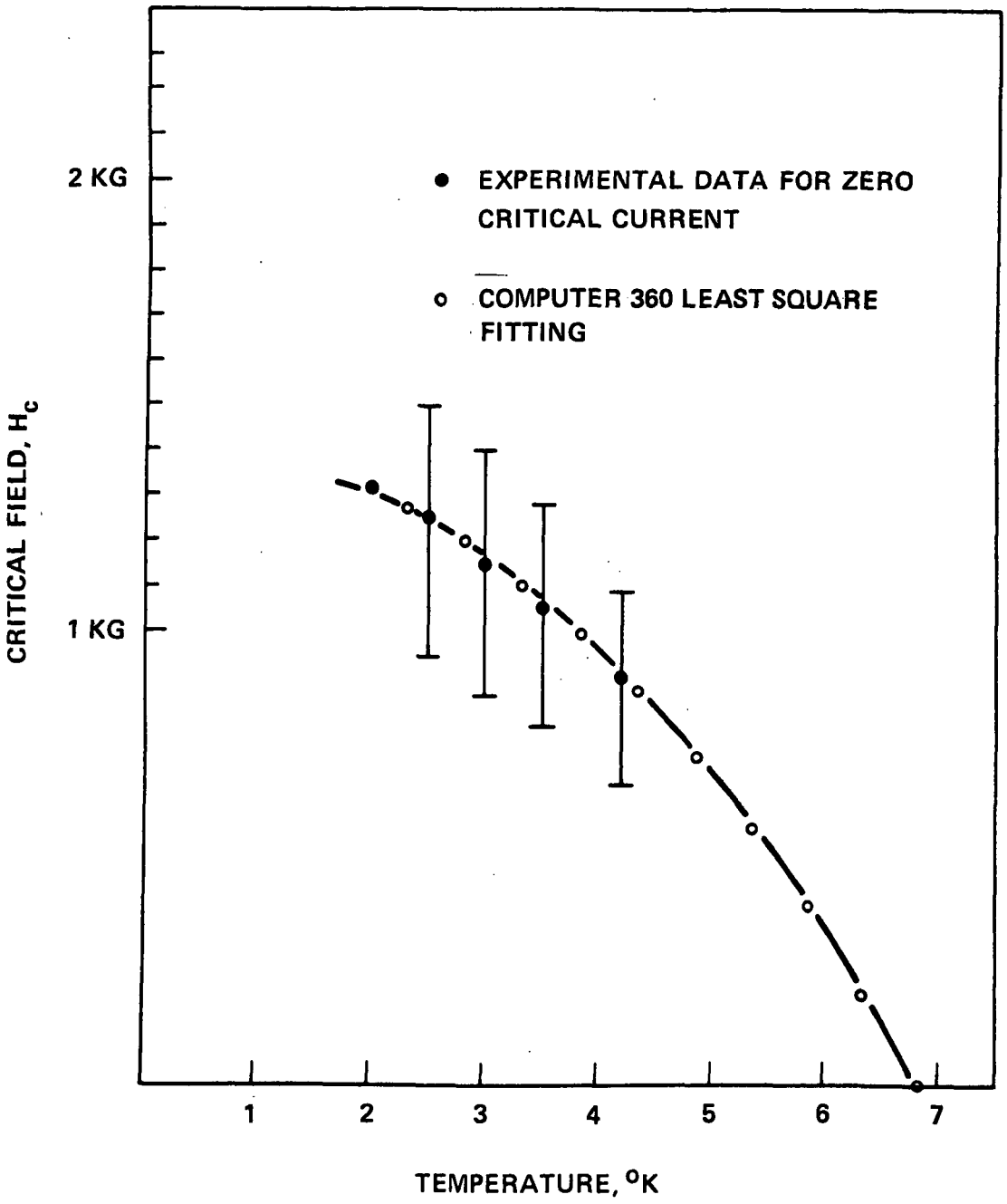

Figure 18. The Critical Field as a Function of Temperature

4. DISCUSSION

4.1 Eutectic Microstructure

The microstructure of the directionally solidified Ni-Ni_3Ta eutectic had a rod-like Ni_3Ta phase in a matrix of α - solid solution Ni. No significant improvement in microstructural alignment was obtained by varying the solidification rate.

The increase in volume fraction of the Ni_3Ta phase in the eutectic is attributed to the diffusion of tantalum to the Ni_3Ta phase. This can be explained by the Fig. 1.

When a tube of rectangular cross section of eutectic liquid of composition C_E is solidified unidirectionally, a eutectic mixture consisting of α - solid solution Ni matrix and Ni_3Ta intermetallic fibers is nucleated and grown from the eutectic liquid at a temperature T_1, as indicated in Fig.1, which is lower than the eutectic temperature T_E (1360^oC). The amount of undercooling needed to nucleate and grow the eutectic mixture is ($T_E - T_1$). A schematic drawing showing the initial growth of a thin layer of fiberlike eutectic mixture is given in Fig.19. A water-cooled copper block is placed at the end of a eutectic mixture of composition C_E for two purposes:

(i) A steep temperature gradient is established between the advancing liquid-solid interface and the initial interface as indicated in Fig. 19 to promote thermal diffusion of the solute atoms in the matrix.

(ii) The extraction of heat from the liquid phase to the solid mixture is unidirectional so that the grown-in fibers may

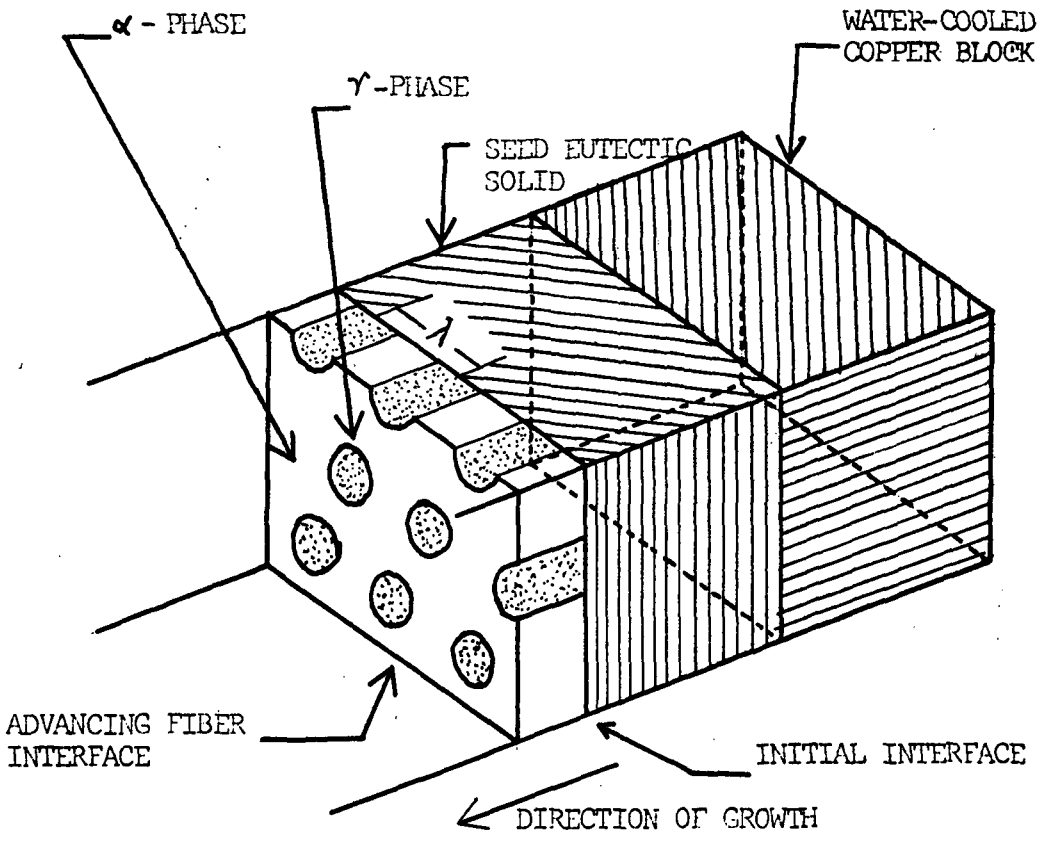

Figure 19. The Steady State Solid-Liquid Interface of a Schematic Fiber-Like Eutectic

19

be perpendicular to the liquid-solid interface as depicted in Fig.19. To simplify the solid state growth process, we consider the growth of a single fiber in the y-direction as illustrated in Fig.20 for six various stages. At stage (1), the α_1 solid solution is in equilibrium with γ intermetallic at temperature T_1 as indicated in Fig. 20(a). I_i, I_a and d_i are initial solid-liquid interface, the advancing interface and the initial diameter of the fiber, respectively. The corresponding temperature and concentration distribution in the α phase and in the x-direction are T(x,0) and C(x,0) as shown in Figs. 20(b) and (c). λ is the inter-particle distance. As growth proceeds from stage (1) to stage (2), the composition of the initial strip α_1 (Fig15(a)(1) changes to α_2 (fig.20(a)(2)) because the temperature descends from T_1 to T_2. Under this condition the supersaturated Ta atoms diffuse to the pre-existing fibers under the influence of a radial concentration gradient dc/dr. Those near the fiber diffuse to the fiber faster than those far away from it because the diffusion distance is shorter. Consequently, a concentration gradient is generated in the y-direction of the matrix at each diffusion temperature. At temperature T_1, the weight percentage of the intermetallic is $\frac{a}{(a+b)}$ as shown in Fig.1. Knowing the crystal structure and density of the Ni_3Ta intermetallic, its volume fraction can be calculated. As the eutectic mixture continues to cool slowly from T_1 to T_5 the matrix changes its composition from α_1 to α_5 which is depleted in Ta in comparison with α_1. At T_5, weight percent of the Ni_3Ta intermetallic is $\frac{c}{(c+b)}$ which is much greater than $\frac{a}{(a+b)}$. As a result, the volume fraction of the Ni_3Ta intermetallic increases as the temperature of the eutectic mixture decreases from T_1 to T_5. Under the combines effect of temperature and concentration gradients, the supersaturated Ta atoms diffuse to the pre-existing fibers, thereby increasing the fiber diameter from d_i to d_f and the volume fraction

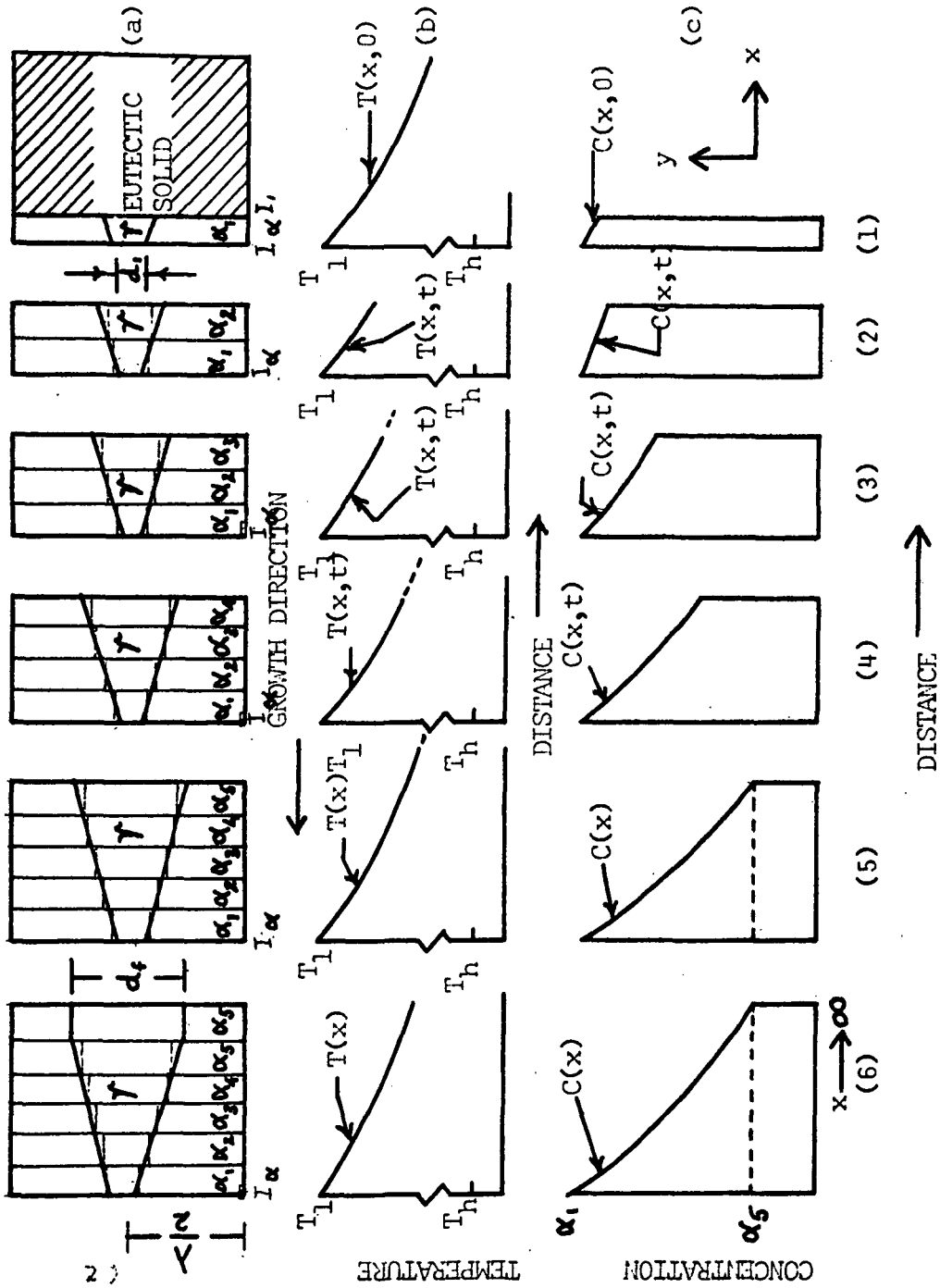

(a) Growth Stages and Shapes of a γ-Phase Filament in Equilibrium with the α-Phase Matrix
(b) Temperature Distribution Along the Length of the Solidified Eutectic Mixtures at Various Growth Stages
(c) Solute Distribution Along the Length of the α-Phase Solid Solution Matrix at Various Growth Stages

Figure 20. Growth of a Single Fiber in the Y-Direction for Various Growth Stages

from $\frac{a}{(a+b)}$ to $\frac{c}{(c+b)}$, epitaxially. At any temperature below T_5, it is assumed that the diffusion process is ineffective. Therefore, the supersaturated Ta atoms are present in the matrix as random precipitates, similar to those in age hardening alloys.

4.2 Tensile Properties

The low strength of the Ni_3Ta phase may be explained by a mechanism which has been applied to other alloy systems to explain their mechanical behaviour [17]. The presence of solute (Ta) atoms in the intermetallic phase can be considered equivalent to the introduction of point defects into the lattice. The lattice strains, induced by microsegregation of solute atoms would lead to the generation of dislocations causing plastic flow to occur at small strain levels, It is also possible that residual stresses, set up upon cooling from the eutectic temperature may generate dislocations in both phases of the alloy. In either case; once dislocations have been introduced into the Ni_3Ta rods, it is expected that the strength of that phase would be sufficiently lowered.

The stress-strain curves show the usual drop in level with rise in temperature, it also flattens out because of reduced strain hardening. Temperature has a large effect on the strain hardening rate of FCC metals. The stress-strain curves shown in Fig. 9 are steeper at room temperature than at higher temperatures. At elevated temperatures the thermal recovery is high and the effective rate of work hardening is much lower.

Tensile tests of Ni-30 wt pct Ta produced some interesting features. Both are samples, Table II, showed an average yield strength of 50.5×10^3 psi. The samples showed an average elongation of about 41 pct at room temperature. This could be indicative of superplastic deformation which is mostly prevalent in eutectic and eutectoid mixtures under tension at elevated temperatures.

TABLE II

Mechanical Properties of Ni - 30 wt pct Ta Alloy

Sample and History	Type of Test	Temperature of Test	Ultimate Tensile Strength, 10^3 psi	0.2 % Off Set Yield Strength, 10^3 psi	Fracture Strain, Percent
Solidified with water cooling at 0.35 in./hr	Tension	Room Temperature	100.10	47.5	41.0
Solidified with water cooling at 0.35 in./hr	Tension	Room Temperature	112.10	60.5	34.0

The occurrence of superplasticity at room temperature in a solid solution alloy is a new phenomenon.

The fracture occurred with practically no necking. One of the samples broke with a knife edge fracture indicating a single crystal.

4.3 Superconducting Property

Since the experimentally determined critical temperature of the unidirectionally solidified Pb-Sn eutectic was $7.37 \pm 0.20^{\circ}K$ which is higher than that of Pb ($7.19^{\circ}K$) and that of Sn ($3.72^{\circ}K$), it is reasonable to assume that the Pb-Sn eutectic is a type II superconductor. To substantiate the above statement, it was decided to determine the relationship between the sample voltage and the external magnetic field. The experimental results yielded a broad and reversible transition from a superconducting to a normal state. However, to establish an affirmative bases for type II superconductor, it is necessary that a magnetization curve for the Pb-Sn eutectic be determined.

5. SUMMARY

5.1 Summary

Unidirectionally solidified Ni-Ni_3Ta eutectic samples were produced by the electron beam floating zone melting technique and were tested in tension and creep. The presumed rodlike, microstructural elements were not aligned parallel with the growth direction, indicating that the nickel solid solution phase and the Ni_3Ta phase may have a high entropies of melting [18].

Under tension, the material behaved in a brittle manner at room temperature and these are very little elongation at higher temperatures.

The nickel-base alloy containing 30 wt pct Ta showed exceptionally high elongation, indicative of superplastic behaviour at room temperature.

The Pb-Sn eutectic behaved as type II superconductor.

BIBLIOGRAPHY

1. McDanels, D.L., R.W. Jech and J.W. Weeton, "Metal Reinforced with Fibers." Metal Progress, 78:118-121 (December, 1960).

2. Jech, R.W., E.P. Weber and A.D. Schwope, "Reactive Metals," Met. Soc. Conf., New York, Interscience Publishers, 109, (1959).

3. Sutton, W.H. and J. Chrone, Fiber Composite Materials, Metals Park, Ohio, Am. Soc. Metals, 163, (1965).

4. Signorelli, R.A., D.W. Petrasek and J.W. Weeton, Modern Composite Materials, L.J. Broutman and R.H. Krock, eds., Menlo Park, California, Addison-Wesley, 146, (1967).

5. Chadwick, G.A., "Eutectic Alloy Solidification." Prog. Matl. Science, 12:99-180 (1963).

6. Chadwick, G.A., "Solidification of $CuAl_2$-Al Eutectic Alloys." J. Inst. Metals, 91:169-173 (1963).

7. Yue, A.S., "Microstructure of Magnesium-Aluminum Eutectic." Trans. TMS-AIME, 224:1010-1015 (1962).

8. Salkind, M.J. and F.D. Lemkey, "Metals with Grown-in Whiskers." Int. Sci. & Tech., 61-66:52-64 (March, 1967).

9. Lemkey, F.D. and R.W. Kraft, "Tensile testing technique for submicron specimens." Rev. Sci. Instr., 33:846-849 (1962).

10. Yue, A.S., F.W. Crossman, A.E. Vidoz and M.I. Jacobson, "Controlled Microstructure of Al-$CuAl_2$ Eutectic Composites and Their Compressive Properties." Trans. TMS-AIME, 242:2441-2452 (1968).

11. Kraft, R.W., "Crystallography of equilibrium phase interface in Al-$CuAl_2$ eutectic alloys." Trans. TMS-AIME, 224:65-75 (1962).

12. Salkind, M.J., F.D. Lemkey, F. George and B.J. Bayles, "Eutectic Composites by Unidirectional Solidification." SAMPE, 10:F35-F44 (1966).

13. Bayles, B.J., J.A. Ford and M.J. Salkind, "The Effect of Elevated-Temperature Exposure on the Microstructure and Tensile Strength of Al_3Ni Whisker-reinforced Aluminum." Trans. TMS-AIME, 239:844-849 (1967).

14. Golasso, F.S., F.C. Douglass, W. Darby and J.A. Batt, "Characterization of the Fe-Fe_xSb Eutectic System with Respect to

Structure and Ferromagnetic roperties." J. Appl. Phys., 38:3241-3244 (1967).

15. Yue, A.S., "Decanted Interface Morphology of Mg-32 wt pct utectic." Trans. TMS-AIME, 227:64-69 (1963).

16. Kraft, R.W., "Controlled Eutectics." J. Metals, 18:192-200 (1966).

17. Wood, D.L., and J.H. Westbrook, "Tensile Behavior of the Intermetallic Compound AgMg." Trans. TMS-AIME, 224:1024-1037 (1962).

18. Jackson, K.A. and J.D. Hunt, "Binary Eutectic Solidification." Trans. TMS-AIME, 236:843-852 (1966).